



International Journal of Pharmacology

ISSN 1811-7775

science
alert

ansinet
Asian Network for Scientific Information



Research Article

Inhibitory Activity of *Balanites aegyptiaca* Phytochemicals on Main Protease of SARS-CoV-2: Virtual Screening and Molecular Dynamics Simulation

Isam Abu Zeid

Department of Biological Sciences, Faculty of Sciences, King Abdulaziz University, Saudi Arabia

Abstract

Background and Objective: SARS-CoV-2 is the virus causing COVID-19, which is a potentially fatal illness. COVID-19 is a severe worldwide public health pandemic, because of its high fatality rate, quick transmission and lack of treatments. This work was carried out to assess the *in silico* inhibitory effect of phytochemicals from *Balanites aegyptiaca* on COVID-19. **Materials and Methods:** In this study *Balanites aegyptiaca* active compounds were screened for their potential activity on the main protease of SARS-CoV-2 using molecular docking and Molecular Dynamic (MD) simulation studies. **Results:** Precose compound showed the best docking energy (-9 kcal mol^{-1}), the best stable complex with the main protease of SARS-CoV-2, MD simulation and stable integration of key residues (His41, Glu166 and Asp189) of the main protease active sites with Precose. **Conclusion:** These findings suggest that this compound could be a good candidate for developing and manufacturing an anti-SARS-CoV-2 medication.

Key words: *Balanites aegyptiaca*, phytochemicals, protease, covid-19, *in silico*, anti-SARS-CoV-2

Citation: Zeid, I.A., 2021. Inhibitory activity of *Balanites aegyptiaca* phytochemicals on main protease of SARS-CoV-2: Virtual screening and molecular dynamics simulation. Int. J. Pharmacol., 17: 482-490.

Corresponding Author: Isam Abu Zeid, Department of Biological Sciences, Faculty of Sciences, King Abdulaziz University, Saudi Arabia Tel: +966556135022

Copyright: © 2021 Isam Abu Zeid. This is an open access article distributed under the terms of the creative commons attribution License, which permits unrestricted use, distribution and reproduction in any medium, provided the original author and source are credited.

Competing Interest: The author has declared that no competing interest exists.

Data Availability: All relevant data are within the paper and its supporting information files.

INTRODUCTION

A deadly corona illness was discovered in Wuhan, China, around the end of 2019¹. In a short period, the disease had spread over the world. The COVID-19 disease had gained prominence and on 11 March, 2020, it was declared a global pandemic². The rapid dissemination of COVID-19 across the world has resulted in an emergency for the global health care system. In many countries, this disease has a varying effect depending on its cultural values, prevention efforts and health infrastructure. Because of the high mortality associated with corona disease, it is challenging for the whole world either to develop new antiviral medications or to improve the existing antiviral drugs to develop an efficient therapeutic solution for COVID-19. It takes years to establish effective drugs that would impede the control of this pandemic. Efficient treatment of control mechanisms to prevent coronavirus must therefore be established³.

For centuries, natural resources have been the main source of remedy and they will continue to be so in the future. In several cultures across the globe, medicinal plants have been the main cure for sickness and the promotion of general health⁴. Natural products are cheap, more reliable and have few or no side effects than synthetic medicines^{5,6}. Desert date (*Balanites aegyptiaca*), is one of the possible and promising herbal medicine that could be included in the healthcare program of many developing countries. The plant can be found in the majority of the world's tropical regions. It is indigenous to most middle East, Africa, Pakistan and Southern Asia^{7,8}.

Traditional healers in many countries utilize different parts of *Balanites aegyptiaca* in folk medicine because they contain anti-diabetic^{8,9}, anti-microbial^{10,11}, antioxidant^{12,13}, anti-cancer^{14,15}, anti-viral^{16,17}, anti-nociceptive and anti-inflammatory^{18,19} and anti-cholesterol²⁰ activities. The fruit of the desert date contains a considerable quantity of sugars²¹. The kernel contains proteins²², polyphenols²³ and nutritive oil, both saturated and unsaturated fatty acids^{22,24}. The most important biochemical components in the fruit of *Balanites aegyptiaca* fruit are saponins²⁵. In addition, the roots, branches and leaves of the desert date contain alkaloids, flavonoids, tannins and vitamins²¹.

Among the many clinical trials currently underway to investigate potential treatments and other viral targets, the major protease (also known as 3CLpro or Mpro) is one of the effective characterized therapeutic targets^{26,27}. The main protease of the novel coronavirus SARS CoV-2 is one of the most efficient targets for antiviral pharmaceutical treatments against COVID-19²⁷. It is necessary for the processing of viral

RNA-encoded polyproteins²⁸. This research was undertaken to assess the *in silico* inhibitory effect of phytocompounds from *Balanites aegyptiaca* against COVID-19.

MATERIALS AND METHODS

Study time: This work was carried out between March and December, 2020, that's Covid-19 pandemic time.

Protein models selection and preparation: The main protease of SARS-CoV-2 proteins was selected as a target for molecular docking and molecular dynamics simulation study, due to its critical involvement in the processing of polyproteins²⁸. The RCSB PDB database had been used to obtain the 3D structure of the main protease (5RFS)²⁹. Then it was prepared for docking by atom protonation, water molecules removal, atom fixation and energy minimization by the Schrödinger Maestro software using Protein Preparation Wizard SiteMap. The Receptor Grid generation was used for the prediction of protein active site, the active site residues were determined according to a previous publication²⁸.

Ligand selection and preparation: Active compounds of *Balanites aegyptiaca* were selected from a previous publication³⁰, the top 11 compounds selected for molecular docking and their 2D structures were obtained from the PubChem database. LigPrep wizards of Schrödinger Maestro software was used for ligands preparation.

Molecular docking: The ligand docking of Maestro was used for molecular docking studies. The protein was set as rigid while ligands were flexible. Extra Precision (XP) docking was used, the partial charge cutoff was set at 0.15 and the van der Waals radii scaling factor was set at 0.8. Post docking energy minimization step was done and only 5 poses per ligand were included. The protein and ligands-interaction were analyzed with PLIP web server³¹, hydrogen bond distances were estimated and interacted residues were specified.

Molecular dynamic simulation: D simulation was done for the complex of Precose and main protease which showed the best docking score. The Desmond package in the Schrödinger Maestro software³² was used for the simulation study. The complex was run at 50 ns MD simulation, TIP3P water model was prepared using a system builder, the system was minimized at 2000 iterations, NPT temperature was set at 300 K, then Maestro was used for visualization of trajectories.

RESULTS AND DISCUSSION

Active sites prediction: The following residues 25, 26, 27, 39, 40, 41, 49, 141, 142, 143, 144, 145, 163, 164, 165, 166, 167, 168, 181, 187, 188, 189, 190 and 404 were identified by SiteMap as the active site of the protein. With a site score of 1.016, the identified pocket indicates its good durability, usual values between 0.5 and 1.0 indicate a binding pocket as drug able site³³. A good drug target has a high durability score and can induce a therapeutic effect in a live system through small-molecule binding.

Molecular docking observations: After molecular docking of the prepared ligand (n = 11) into protein active sites, different docking energies and conformations were generated, Precose (CID_444254) showed docking score -9, Meptazinol hydrochloride (CID_65483) showed docking score -5.3, 1 α , 25-dihydroxy-3 (CID_9953732) showed docking score -4.8 and Hyocholic acid (CID_92805) showed -4.3 in Table 1 and Fig. 1. Precose (CID_444254) showed the highest docking score (-9 kcal mol⁻¹) and interaction with SARS-CoV-2 main protease protein as shown in Table 1 and Fig. 2. The Precose compounds (CID_444254) is also known as

title 444254 docking score -9.047	title 65483 docking score -5.338	title 9953732 docking score -4.761	title 92805 docking score -4.266
title 6291 docking score -4.262	title 2576 docking score -3.782	title 5280453 docking score -3.608	title 26133 docking score -3.594
title 5484727 docking score -3.0	title 193872 docking score -2.546	title 5484727 docking score -1.75	title 5282181 docking score -1.257

Fig. 1: 2D structures of the selected *Balanites aegyptiaca* compounds with their docking score and PubChem IDs

Table 1: PubChem ID and docking score of the selected compounds from the *Balanites aegyptiaca*

Compounds	ID	Docking score	H-bonds
Precose	CID_444254	-9.0	His41, His164, Gln189, Thr190
Meptazinol hydrochloride	CID_65483	-5.3	His41
1 α , 25-dihydroxy-3 EDIT NAME	CID_9953732	-4.8	Gly143, Thr190
Hyocholic acid	CID_92805	-4.3	Gly143
Mestranol	CID_6291	-4.3	Asn142
Carisoprodol	CID_2576	-3.9	Glu166, Asn142
Calcitriol	CID_5280453	-3.6	Gly143
Hydrocortisone butyrate	CID_26133	-3.6	Glu166, His164, Cys145
Trandolapril	CID_5484727	-3.0	His41, Glu166
Methyl N-(a-methylbutyryl) glycine	CID_193872	-2.5	Cys145
Alfalcidol	CID_5282181	-1.3	Gln189

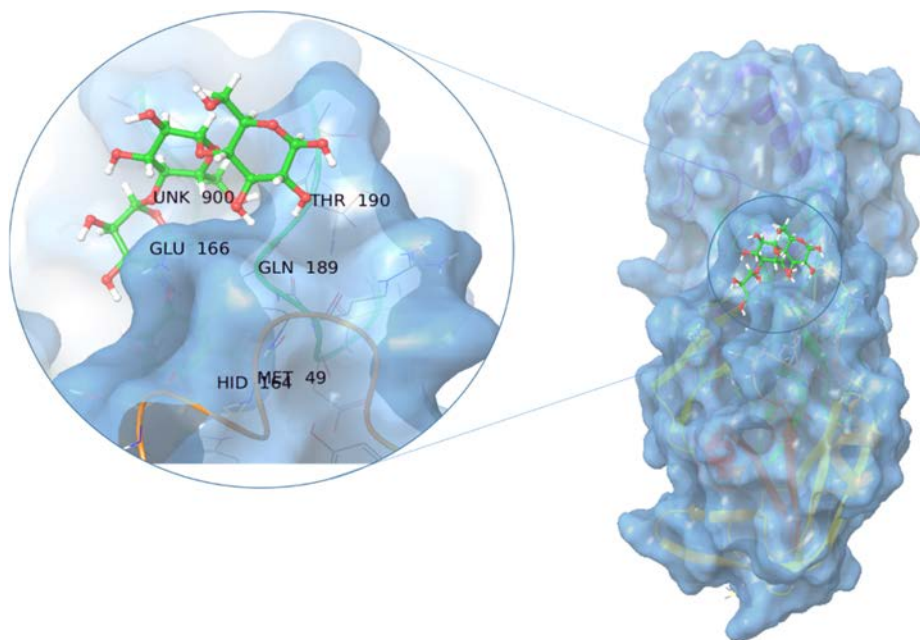


Fig. 2: 3D interaction of the precose compound (green) with the main protein of SARS-CoV-2 (blue)
Enlarged view showing the residues associated with ligand interaction

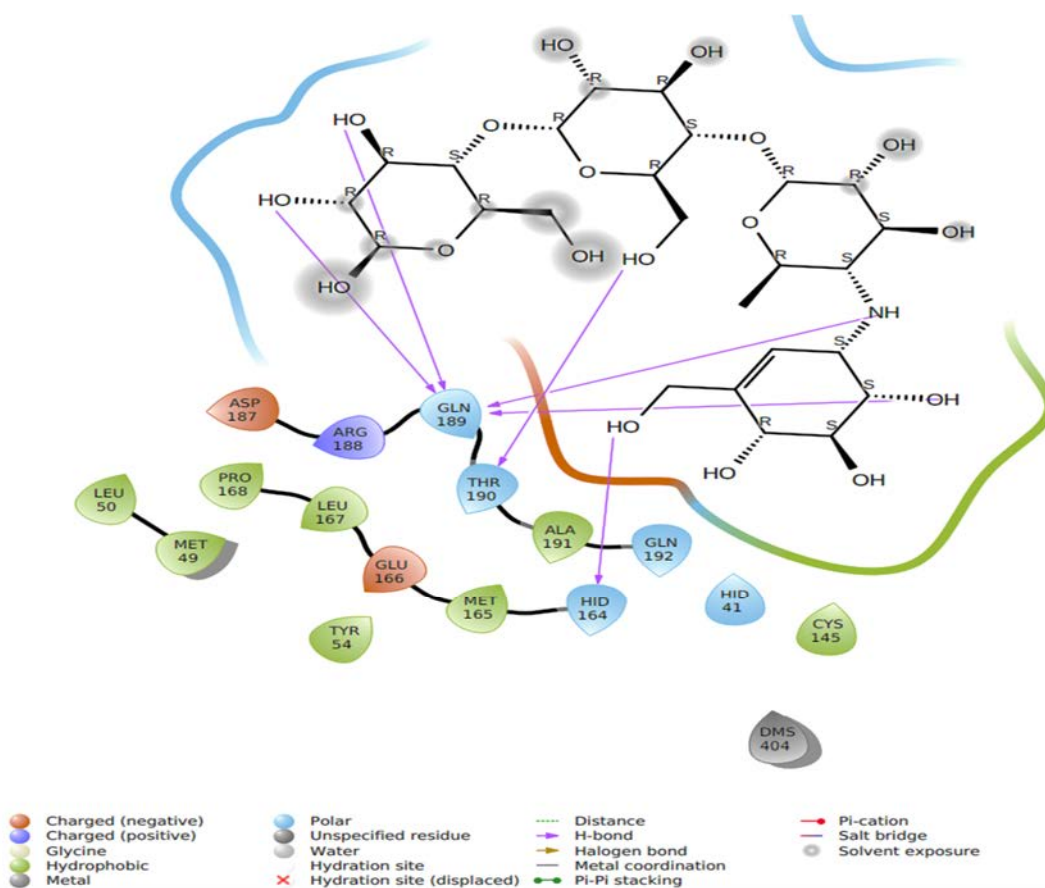


Fig. 3: 2D interaction of the precose compound with main residues of SARS-CoV-2
Hydrogen bonds are shown in purple arrows

Table 2: H-bonds formation by the interaction of main protease residues with Precose compound

Insert	Residue	AA	Distance H-A	Distance H-A	Donor angle	Donor atom	Acceptor atom
1	41A	HIS	2.96	3.77	143.71	4741 [O3]	614 [Nar]
2	164A	HIS	1.88	2.81	162.61	4746 [O3]	2527 [O2]
3	189A	GLN	2.71	3.64	162.97	4738 [O3]	2899 [O2]
4	189A	GLN	1.94	2.9	174.24	4743 [O3]	2895 [O2]
5	189A	GLN	2.05	2.93	150.66	4740 [O3]	2895 [O2]
6	189A	GLN	3.23	3.64	107.61	4733 [O3]	2899 [O2]
7	189A	GLN	2.35	3.34	166.38	4747 [N3]	2899 [O2]
8	190A	THR	2.5	2.93	105.24	2909 [Nam]	4742 [O3]
9	190A	THR	1.72	2.68	168.41	4742 [O3]	2912 [O2]

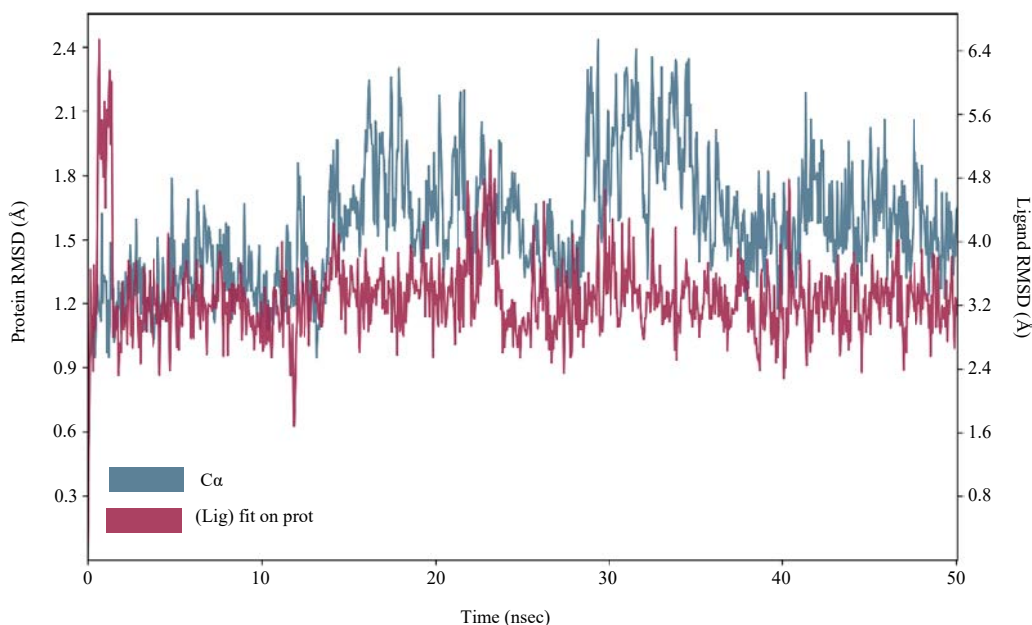


Fig. 4: Root mean square deviations (RMSDs) trajectories of the main protease of SARS-CoV-2 residues and Precose complex run at 50 ns

Protein backbones carbon alpha atoms showed in blue colour and the ligand in red colour

anti-hyperglycemia agents, which are clinically applied to prolong the increases in post-meal blood glucose³⁴. *Balanites aegyptiaca* compounds used in this study have the potential activity against the COVID-19³⁵.

This good docking energy was the result of the good positioning of the ligand in the protein active site. Results showed the nine hydrogen bonds, which were formed due to the interaction of Precose and the main of SARS-CoV-2, His41 formed a stable hydrogen bond with a distance of 2.96 Å, four hydrogen bonds were observed with Gln189, which is located at the centre of the binding site located between Gln-189 and Glu-166 in Fig. 3. Table 2 summarizes hydrogen bonding (H-bond), hydrogen-acceptor atom distance (H-A) and donor-acceptor atom distance (D-A). The main protease residues GLN189 formed five H-bonds with the ligand acceptor atom number 2895, with distances

ranging from 2.8-3.6 Å. Additionally, THR190 established two strong hydrogen bonds and two acceptor atoms (4742 O3 and 2912 O2) that are involved in the ligand interaction. These findings are consistent with those of Abel *et al.*³⁶, who identified the same response of natural chemicals with Gln_189, Glu_166 residues of the main protease. Furthermore, in another study, the same residues were found to have the same interaction with other active compounds³⁷. However, the main protease residues such as Ser_284, Thr_285 and Ile_286 have not been linked to our compound's interaction²⁸.

The Precose compound can block the main protease active site's catalytic residues containing the conserved catalytic residues His_41 and Cys_145³⁸. The His_41 is located at S2 subunits, which have an essential role in performing good binding with hydrophobic groups³⁹. The

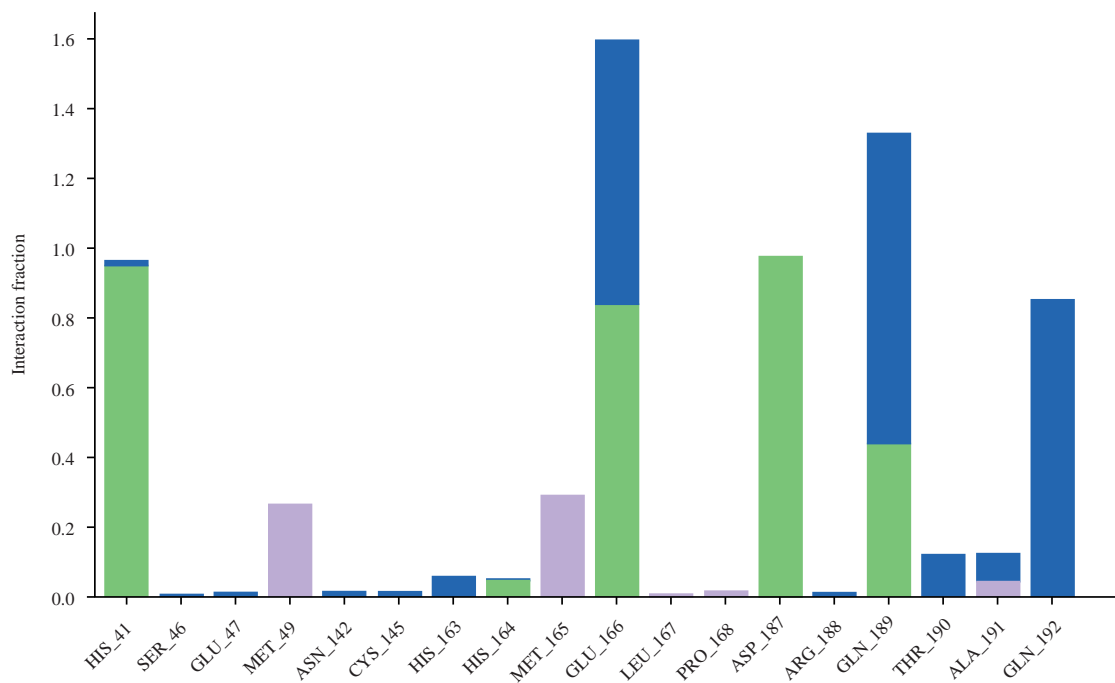


Fig. 5: Frequencies of the interactions of the protein with the ligand throughout the 50 ns simulation time
 Graph showed the number of times for a specific reaction is maintained (e.g., a value of 0.25 refers to 25%), green colour indicated the H-bonds while the blue colour showed the water bridges and the violet colour demonstrated the hydrophobic interaction

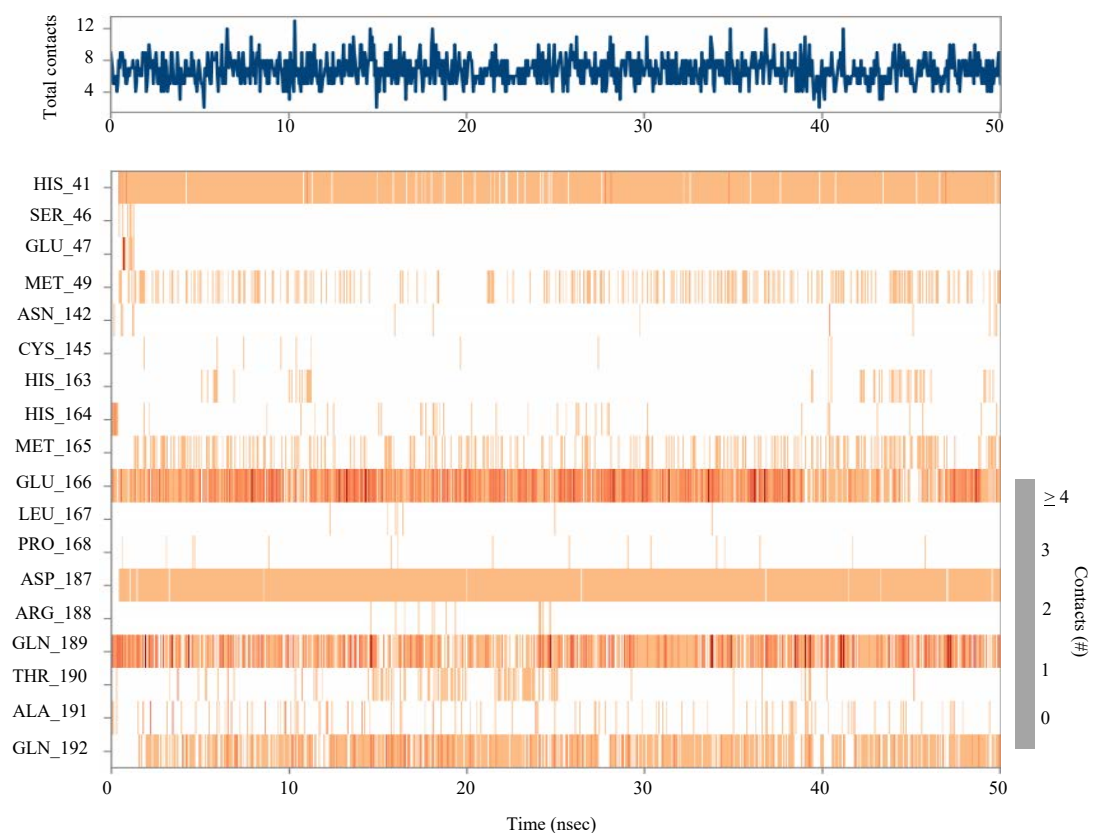


Fig. 6: Interactions and bond types formed between ligand and protein during the simulation time (50ns)

blocking of His41 could result in loss of main protease enzyme activity. The two stable hydrogen bonds were formed with Thr_190 with small distances of 2.5 and 1.7 Å (Table 2). This essential residue Thr_190 located at S4 of the enzyme binding pocket³⁹.

Observation of molecular dynamic simulation: The strength of Precose compound binding affinities with the active site residues of the main of SARS-CoV-2 was assessed using a molecular dynamics simulation. This compound showed good binding affinity to protein backbones residues during 50 ns simulation time in Fig. 4. The ligand remains intact to protein backbones during the whole simulation time from 2 ns until the end of the simulation. The fluctuation of the complex remains in a range from 0.6-2.4 Å. This means good stability, usually, fluctuation in this range considered stable^{40,41}. Residues showed integration persisted for more than 70% in simulation considered stable (Desmond), in the current study, three residues (His41, Glu166 and Asp189) showed stable H-bonds with the ligand. Additionally, Glu166, Gln189 and Gln192 showed stable water bridges in Fig. 5 and 6. The previous study also showed that stable blocking of the key residues His41, Glu166 was located at the active site of the enzymes³⁹ which may prevent the essential role of the main protease in SARS-CoV-2 polyproteins processing²⁸.

CONCLUSION

The computational methods are widely used for the prediction of SARS-CoV-2 inhibitors 35, 37, 38. In this study, a total of 12 *Balanites aegyptiaca* compounds were screened for their possible activity on SARS-CoV-2 main protease. Based on docking energy, number and types of bonds in addition to the positioning of ligands on protein active site, the precise molecule was identified as the best inhibitor of the main protease. The binding affinity of this compound to the main protease was confirmed by MD simulation. These results provide an insight for future *in vitro* or *in vivo* studies that sheds light on the possible use of precision in the treatment of SARS-CoV-2 and similar viral diseases. Further studies are required to confirm the usefulness of these novel findings.

SIGNIFICANCE STATEMENT

This study identified the Precose molecule as the inhibitor of the main protease of SARS-CoV-2 that can be beneficial for

further *in vitro* or *in vivo* research into the possible use of it in the treatment of SARS-CoV-2 and other viral diseases.

REFERENCES

1. Baloch, S., M.A. Baloch, T. Zheng and X. Pei, 2020. The coronavirus disease 2019 (COVID-19) pandemic. *Tohoku J. Exp. Med.*, 250: 271-278.
2. Cucinotta, D. and M. Vanelli, 2020. Who declares COVID-19 a pandemic. *Acta BioMed.: AteneiParmensis*, 91: 157-160.
3. Joshi, T., T. Joshi, P. Sharma, S. Mathpal, H. Pundir, V. Bhatt and S. Chandra, 2020. *In silico* screening of natural compounds against COVID-19 by targeting Mpro and ACE2 using molecular docking. *Eur. Rev. Med. Pharmacol. Sci.*, 24: 4529-4536.
4. Jamshidi-Kia, F., Z. Lorigooini and H. Amini-Khoei, 2018. Medicinal plants: Past history and future perspective. *J. Herbmmed Pharmacol.*, 7: 1-7.
5. Kooti, W., M. Farokhipour, Z. Asadzadeh, D. Ashtary-Larky and M. Asadi-Samani, 2016. The role of medicinal plants in the treatment of diabetes: A systematic review. *Electron. Phys.*, 8: 1832-1842.
6. Verma, S., M. Gupta, H. Popli and G. Aggarwal, 2018. Diabetes mellitus treatment using herbal drugs. *Int. J. Phytomed.*, Vol. 10. 10.5138/09750185.2181.
7. Elfeel, A.A., 2012. Effect of seed pre-treatment and sowing orientation on germination of *Balanites aegyptiaca* (L.) Del. *Seeds. Agric. J.*, 7: 191-193.
8. Rashad, H., F.M. Metwally, S.M. Ezzat, M.M. Salama, A. Hasheesh and A.A. Motaal, 2017. Randomized double-blinded pilot clinical study of the antidiabetic activity of *Balanites aegyptiaca* and UPLC-ESI-MS/MS identification of its metabolites. *Pharm. Biol.*, 55: 1954-1961.
9. Abou Khalil, N.S., A.S. Abou-Elhamd, S.I. Wasfy, I.M. El Mileegy, M.Y. Hamed and H.M. Ageely, 2016. Antidiabetic and antioxidant impacts of desert date (*Balanites aegyptiaca*) and Parsley (*Petroselinum sativum*) aqueous extracts: Lessons from experimental rats. *J. Diabetes Res.* Vol. 2016. 10.1155/2016/8408326.
10. Doughari, J.H., M.S. Pukuma and N. De, 2007. Antibacterial effects of *Balanites aegyptiaca* L. Drel. and *Moringa oleifera* Lam. on *Salmonella typhi*. *Afr. J. Biotechnol.*, 6: 2212-2215.
11. Abdulhamid, A. and I. Sani, 2016. Preliminary phytochemical screening and antimicrobial activity of aqueous and methanolic leaf extracts of *Balanites aegyptiaca* (L.). *Int. Res. J. Pharm. Biosci.*, 3: 1-7.
12. Montasser, A.O.S., H. Saleh, O.A. Ahmed-Farid, A. Saad and M.A.S. Marie, 2017. Protective effects of *Balanites aegyptiaca* extract, melatonin and ursodeoxycholic acid against hepatotoxicity induced by methotrexate in male rats. *Asian Pacific J. Trop. Med.*, 10: 557-565.

13. Issa, N.M., F.K. Mansour, F.A. El-Safti, H.Z. Nooh and I.H. El-Sayed, 2015. Effect of *Balanites aegyptiaca* on ehrlich ascitic carcinoma growth and metastasis in Swiss mice. Exp. Toxicol. Pathol., 67: 435-441.
14. Hassan, L.E.A., S.S. Dahham, S.A.M. Saghir, A.M.A. Mohammed, N.M. Eltayeb, A.M.S.A. Majid and A.S.A. Majid, 2016. Chemotherapeutic potentials of the stem bark of *Balanite aegyptiaca* (L.) Delile: An antiangiogenic, antitumor and antioxidant agent. BMC Complementary Alter. Med., Vol. 16. 10.1186/s12906-016-1369-5.
15. Yassin, A.M., N.M. El-Deeb, A.M. Metwaly, G.F. El Fawal, M.M. Radwan and E.E. Hafez, 2017. Induction of apoptosis in human cancer cells through extrinsic and intrinsic pathways by *Balanites aegyptiaca* furostanol saponins and saponin-coated silver nanoparticles. Applied Biochem. Biotechnol., 182: 1675-1693.
16. Al Ashaal, H.A., A.A. Farghaly, M.M. Abd El Aziz and M.A. Ali, 2010. Phytochemical investigation and medicinal evaluation of fixed oil of *Balanites aegyptiaca* fruits (Balantiaceae). J. Ethnopharmacol., 127: 495-501.
17. Awad, M.A., R.A. El Dibc, N. Almusayeb, S. Al-Massaranic and K.M.O. Ortashi, 2013. Novel *Balanites aegyptiaca* mesocarp synthesized silver nanoparticles: Formation, characterization, antimicrobial, cytotoxicity and antiviral effects. Dig. J. Nanomater. Biostruct., 8: 1665-1677.
18. Speroni, E., R. Cervellati, G. Innocenti, S. Costa, M.C. Guerra, S. Dall'Acqua and P. Govoni, 2005. Anti-inflammatory, antinociceptive and antioxidant activities of *Balanites aegyptiaca* (L.) Delile. J. Ethnopharmacol., 98: 117-125.
19. Ali, S.A., A.H. Mohamed and G.E. Mohammed, 2014. Fatty acid composition, anti-inflammatory and analgesic activities of *Balanities aegyptiacaseeds* in rats. J. Agric. Vet. Sci., 15: 16-26.
20. Ezzat, S.M., A. Abdel Motaal and S.A.W. El Awdan, 2017. *In vitro* and *in vivo* antidiabetic potential of extracts and a furostanol saponin from *Balanites aegyptiaca*. Pharm. Biol., 55: 1931-1936.
21. Sagna, M.B., K.S. Niang, A. Guisse and D. Goffner, 2014. *Balanites aegyptiaca* (L.) delile: Geographical distribution and ethnobotanical knowledge by local populations in the ferlo (north senegal). Biotechnol. Agron. Soc. Environ., 18: 503-511.
22. Osman-Bashir, N.A. and S.A.A. Elhoussein, 2017. Variability in kernel oil and kernel crude protein contents in Sudanese fruit accessions of *Balanitesaegyptiaca* (L.) del. Pak. J. Sci. Ind. Res. Ser. A: Phys. Sci., 60: 134-140.
23. Ahmed, A.A.O., A. Kita, A. Nemš, J. Miedzianka, R. Foligni, A.M.A. Abdalla and M. Mozzon, 2020. Tree-to-tree variability in fruits and kernels of a *Balanites aegyptiaca* (L.) del. population grown in Sudan. Trees, 34: 111-119.
24. Gardette, J.L. and M. Baba, 2013. FTIR and DSC studies of the thermal and photochemical stability of *Balanites aegyptiaca* oil (toogga oil). Chem. Phys. Lipids, 170-171: 1-7.
25. Yadav, J.P. and M. Panghal, 2010. *Balanites aegyptiaca* (L.) Del. (Hingot): A review of its traditional uses, phytochemistry and pharmacological properties. Int. J. Green Pharm., 4: 140-146.
26. Anand, K., J. Ziebuhr, P. Wadhvani, J.R. Mesters and R. Hilgenfeld, 2003. Coronavirus main proteinase (3CLpro) structure: Basis for design of anti-SARS drugs. Sci., 300: 1763-1767.
27. Estrada, E., 2020. Topological analysis of SARS cov-2 main protease. Chaos: An Interdiscip. J. Nonlinear Sci., Vol. 30. 10.1063/5.0013029.
28. Zhang, L., D. Lin, X. Sun, U. Curth and C. Drosten *et al.*, 2020. Crystal structure of SARS-CoV-2 main protease provides a basis for design of improved α -ketoamide inhibitors. Science, 368: 409-412.
29. Berman, M.H., J. Westbrook, Z. Feng, G. Gilliland and T.N. Bhat *et al.*, 2000. The protein data bank. Nucl. Acids Res., 28: 235-242.
30. Satpute, S.B. and D.J. Vanmare, 2018. Phytochemical analysis of leaf extract of journal of *Balanites aegyptica* L. by HRLC-MS analysis. J. Pharmacogn. Phytochem., 7: 1736-1739.
31. Salentin, S., S. Schreiber, V.J. Haupt, M.F. Adasme and M. Schroeder, 2015. PLIP: Fully automated protein-ligand interaction profiler. Nucleic Acids Res., 43: W443-W447.
32. Vijayalakshmi, P., J. Nisha and M. Rajalakshmi, 2014. Virtual screening of potential inhibitor against FtsZ protein from *Staphylococcus aureus*. Interdiscip. Sci.: Comput. Life Sci., 6: 331-339.
33. Michel, M., T. Visnes, E.J. Homan, B. Seashore-Ludlow and M. Hedenström *et al.*, 2019. Computational and experimental druggability assessment of human DNA glycosylases. ACS Omega, 4: 11642-11656.
34. Chen, T.H., Y.S. Fu, S.P. Chen, Y.M. Fuh, C. Chang and C.F. Weng, 2021. *Garcinia linii* extracts exert the mediation of anti-diabetic molecular targets on anti-hyperglycemia. Biomed. Pharmacother., Vol. 134. 10.1016/j.biopha.2020.11115.
35. Bhuiyan, F.R., S. Howlader, T. Raihan and M. Hasan, 2020. Plants metabolites: Possibility of natural therapeutics against the COVID-19 pandemic. Front. Med., Vol. 7. 10.3389/fmed.2020.00444.
36. Abel, R., M.P. Ramos, Q. Chen, H. Pérez-Sánchez and F. Coluzzi *et al.*, 2020. Computational prediction of potential inhibitors of the main protease of SARS-CoV-2. Front. Chem., Vol. 8. 10.3389/fchem.2020.590263.

37. Abhinand, C.S., A.S. Nair, A. Krishnamurthy, O.V. Oommen and P.R. Sudhakaran, 2020. Potential protease inhibitors and their combinations to block SARS-CoV-2. *J. Biomol. Struct. Dyn.*, : 1-15.
38. Muteeb, G., A. Alshoabi, M. Aatif, M.T. Rehman and M.Z. Qayyum, 2020. Screening marine algae metabolites as high-affinity inhibitors of SARS-CoV-2 main protease (3CLpro): an *in silico* analysis to identify novel drug candidates to combat COVID-19 pandemic. *Appl. Biol. Chem.*, Vol. 63. 10.1186/s13765-020-00564-4.
39. Stoddard, S.V., S.D. Stoddard, B.K. Oelkers, K. Fitts and K. Whalum *et al.*, 2020. Optimization rules for SARS-CoV-2 M^{pro} antivirals: Ensemble docking and exploration of the coronavirus protease active site. *Viruses*, Vol. 12. 10.3390/v12090942.
40. Nemaysh, V. and P.M. Luthra, 2017. Computational analysis revealing that K634 and T681 mutations modulate the 3D-structure of PDGFR- β and lead to sunitinib resistance. *RSC Adv.*, 7: 37612-37626.
41. Khan, M.T., A. Ali, Q. Wang, M. Irfan and A. Khan *et al.*, 2020. Marine natural compounds as potent inhibitors against the main protease of SARS-CoV-2: A molecular dynamic study. *J. Biomol. Struct. Dyn.*, 39: 3627-3637.